ELSEVIER

^{29}Si and ^{17}O NMR Investigation of the Structure of Some Crystalline Calcium Silicate Hydrates

Xiandong Cong and R. James Kirkpatrick
Department of Geology and ACBM Center, University of Illinois at Urbana-Champaign, Urbana

This paper presents the results of a systematic investigation of the structure of ^{17}O-enriched, hydrothermally synthesized 1.1-nm tobermorite, 1.4-nm tobermorite, jennite, calciochondrodite, xonotlite, and hillebrandite, using ^{29}Si magic angle spinning (MAS) NMR, ^{1}H-^{29}Si cross-polarization magic angle spinning (CPMAS) NMR, and ^{17}O MAS NMR. The ^{17}O and most of the ^{1}H-^{29}Si CPMAS results are the first reported for these phases. Six types of oxygen sites were observed in tobermorite and jennite, including both Si-OH and Ca-OH linkages. The structure of 1.4-nm tobermorite is similar to that of 1.1-nm tobermorite with about 26% of the Ca^{2+}'s in the interlayers. The results support the proposed jennite structure in which silicate chains and rows of OH^- groups alternately occur along the CaO layers [1]. Jennite contains long, single silicate chains similar to those in 1.4-nm tobermorite, with Si-OH sites primarily occurring on bridging tetrahedra, and there seems to be no interlayer Ca^{2+}'s. Although the Si sites in xonotlite and calciochondrodite cross-polarize well, neither contains Si-OH linkages. ADVANCED CEMENT BASED MATERIALS 1996, 3, 133–143

KEY WORDS: Jennite, NMR, Tobermorite, Xonotlite

Crystalline calcium silicate hydrates are important minerals to cement science, some having compositions similar to that of calcium-silicate-hydrate (C-S-H) gel, and occurring in cement materials heated at moderate temperatures. The structure of C-S-H has been thought to be similar to those of 1.4-nm tobermorite and jennite [2]. Unfortunately, the structures of the phases of greatest interest to cement science have not been fully determined. Even for 1.1-nm tobermorite, whose structure has been solved [3], there is still controversy about the polymerization and the assignments of the ^{29}Si magic angle spinning (MAS) NMR peaks [4–6].

Address correspondence to: Xiandong Cong, Department of Geology, University of Illinois, 153 Natural History, 1301 West Green Street, Urbana, Illinois 61801.
Received September 1, 1994; Accepted December 12, 1995

ISSN 1065-7355/96/$15.00
PII S1065-7355(96)00022-3

We provide in this paper results of a combined ^{17}O MAS, ^{29}Si MAS, and ^{1}H-^{29}Si CPMAS NMR investigation of the structures of 1.4-nm tobermorite, 1.1-nm tobermorite, jennite, hillebrandite, calciochondrodite, and xonotlite. Although ^{29}Si MAS NMR has been previously used to study some of these phases [4,7–9], data for ^{17}O under high speed MAS and systematic ^{1}H-^{29}Si CPMAS NMR results have not been previously available and shed significant light on the structures of these phases.

Experimental

Sample Preparation

Most of the phases studied in this paper were hydrothermally synthesized with Parr Acid Digestion Bombs (Parr Instrument, Moline, IL) under conditions described in Table 1. Deionized water was used in the synthesis and was bubbled with flowing N_2 gas to eliminate dissolved CO_2. All loading and unloading of the reaction vessels were within a glove bag filled with flowing N_2 gas to prevent carbonation. The solid products were dried under flowing N_2 gas at room temperature.

Both 1.1-nm and 1.4-nm tobermorite are natural minerals and can be synthesized hydrothermally from a variety of starting materials [5,10–12]. A separate 1.1-nm tobermorite specimen was obtained indirectly by heating 1.4-nm tobermorite at 105°C for 12 hours.

Jennite occurs naturally [13,14] and has been hydrothermally synthesized at 80°C for 40–100 days [15]. We used both quartz and acid silica as starting materials with bulk calcium/silica (C/S) ratios between 1.2 and 1.5. When the reactions were terminated after 11 months, only the sample listed in Table 1 was phase-pure jennite, others were mixtures of C-S-H and jennite or 1.4-nm tobermorite depending on the C/S ratio.

Hillebrandite is a natural mineral but is difficult to synthesize [16]. The sample used was kindly provided by Dr. H. Ishida (INAX Corp., Japan), which was hydrothermally synthesized [17].

Advn Cem Bas Mat
1996;3:133–143

The ^{17}O enrichment was achieved via isotopic exchange with 21.8% ^{17}O-enriched $H_2^{17}O$ at water/solid ratios between 2 and 4 for 2–3 days at 10–80°C below the synthesis temperatures. The ^{17}O exchange does not alter the structure of the specimens, as shown by both X-ray diffraction (XRD) and ^{29}Si NMR.

NMR Spectroscopy

^{29}Si MAS NMR spectra were recorded at conditions described elsewhere [18]. Conditions for the ^{17}O MAS NMR spectra were the same as those in ref 19, and those for the ^{1}H-^{29}Si CPMAS NMR spectra the same as in ref 20.

Results and Discussion

1.1-nm Tobermorite

^{29}Si MAS NMR. The ^{29}Si MAS NMR spectrum of the directly synthesized 1.1-nm tobermorite contains three main peaks, corresponding to Q^1 (–79.5 ppm), Q^2 (–85.9 ppm), and Q^3 (–95.7 ppm) Si sites, and possibly two small peaks between the main Q^2 and Q^3 peaks at ca. –89.7 and –92.1 ppm (Figure 1A). In addition, the main Q^2 and Q^3 peaks are not symmetric and contain small shoulders or are broadened on the left side. These results are consistent with those previously reported [4,9].

The ^{29}Si NMR spectrum of 1.1-nm tobermorite obtained by heating 1.4-nm tobermorite at 105°C for 12 hours contains primarily Q^2 sites resonating at *ca.* –85.9 ppm, but the peak is broad, and there is a small shoulder corresponding to Q^1 and Q^3 sites (Figure 1B). This sample is, thus, less polymerized than the directly synthesized one. The full width at half height (FWHH) of the Q^2 peak is approximately 5.3 ppm, compared to ca. 2.5 ppm for the Q^2 peak of the directly synthesized sample. The XRD peaks of the heated sample are also broader. These observations all indicate that the heated sample is less well ordered than the directly synthesized sample.

The average structure of 1.1-nm tobermorite, $Ca_{2.25}[Si_3O_{7.5}(OH)_{1.5}] \cdot H_2O$, has been determined [3] and consists of CaO layers sandwiched between single silicate chains and additional Ca^{2+} and H_2O molecules in the interlayer (Figure 2). There are six crystallographically different Si sites, forming two nonequivalent dreierkettens. The ideal structure contains only Q^2 Si sites, but our results and most published data also

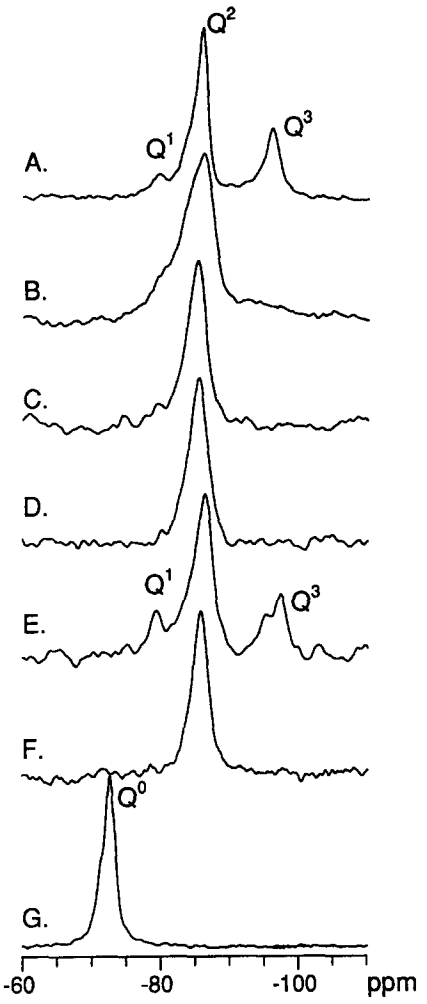

FIGURE 1. ^{29}Si MAS NMR spectra of different phases. A, Directly synthesized 1.1-nm tobermorite; B, 1.1-nm tobermorite by heating 1.4-nm tobermorite at 105°C for 12 hours; C, 1.4-nm tobermorite; D, jennite; E, xonotlite, F, hillebrandite; and G, calciochondrodite.

TABLE 1. Synthesis conditions of the phases investigated

Phase	Starting materials	C/S (molar)	w/s (weight)	Temperature (°C)	Time (days)	XRD phases
Tobermorite (1.1-nm)	CaO, quartz	0.8	5	175	2	pure
Tobermorite (1.4-nm)	CaO, quartz	0.9	20	80	133	pure
Jennite	CaO, acid silica	1.4	20	80	335	pure
Calciochondrodite	CaO, β-C_2S	2.5	3	210	21	contains $Ca(OH)_2$
Xonotlite	CaO, quartz	1.0	7.5	230	5	pure
Hillebrandite[a]						pure

C/S = calcium/silicate; w/s = water/solid; XRD = X-ray diffraction.
[a]Hillebrandite was provided by Dr. H. Ishida (INAX Co., Japan).

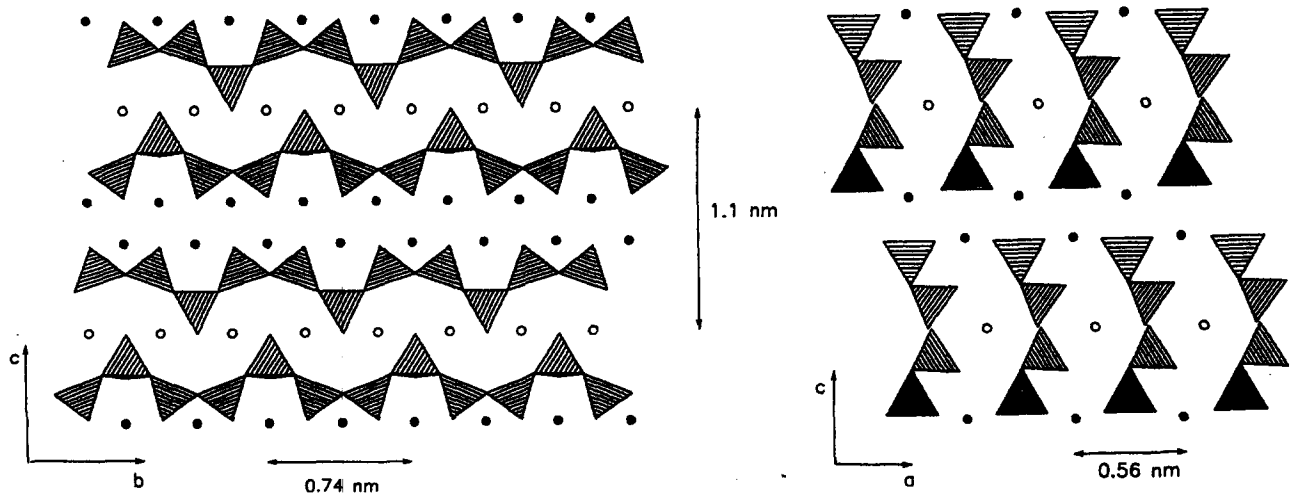

FIGURE 2. Simplified projection of the 1.1-nm tobermorite crystal structure along **a** (left) and **b** (right), with OH^- groups and H_2O molecules omitted (based on ref 3). The filled circles represent Ca^{2+} in central CaO layers and the empty ones represent Ca^{2+} in interlayer sites, which are partially occupied. The tetrahedra close to the central CaO layers appear in pairs and have been termed pairing tetrahedra (PT). Those linking the pairs together in the dreierketten arrangement are called bridging tetrahedra (BT).

show the presence of Q^1 and Q^3 sites. As shown in Figure 2, displacement of one chain by **b**/2 allows the bridging tetrahedra (BT) of two chains to cross-link. The existence of such cross-linking has been considered to be one of the reasons for the so-called anomalous thermal behavior of some 1.1-nm tobermorites, which do not collapse to 0.9 nm-tobermorite upon heating at 300°C [21]. Our directly synthesized 1.1-nm tobermorite maintains its basal spacing upon heating at 315°C for 36 hours, supporting this idea. The 1.4-nm tobermorite sample collapsed to 0.97 nm when heated directly at 315°C for 36 hours, and ^{29}Si MAS NMR indicates that it contains primarily Q^2 sites.

The downfield shoulders on the Q^2 and Q^3 peaks and small peaks between them in the ^{29}Si NMR spectrum of the directly synthesized sample indicate that there are multiple Q^2 and Q^3 Si sites in the structure. As discussed by Hamid [3], there are many mechanisms to produce stacking disorder in 1.1-nm tobermorite, including displacement and tilting of the tetrahedra. Multiple Q^2 and Q^3 sites are, thus, possibly due to distortions caused by structural disorder. These sites may have the same polymerization as the main peak but local structural environments with different, for example, bond angles and bond distances.

It has been thought that not all dreierketten chains in tobermorite are cross-linked by formation of Q^3 sites, and that the Q^2 sites and specifically BT in the uncross-linked chains are responsible for the downfield shoulder on the Q^2 peak [4,5]. These ideas are inconsistent with our observations. In 1.1.-nm tobermorite, only BT can cross-link to form double chains (Figure 2), and thus the maximum relative intensity of the Q^3 peak should be 0.33. The observed relative intensity of the Q^3 peak of our directly synthesized sample is 0.31, indicating that almost all of the BT are cross-linked. However, there is still a relatively large downfield shoulder on the Q^2 peak, and it is impossible that the shoulder is due to Q^2 Si sites in silicate chains that are not cross-linked.

^{1}H-^{29}Si CPMAS NMR. The ^{1}H-^{29}Si CPMAS NMR spectra of 1.1-nm tobermorite are generally similar to the MAS NMR spectra (Figure 3A). All three main peaks, Q^1, Q^2, and Q^3, can be cross-polarized (CP), and their relative intensities vary with contact time. The contact time dependence of the CP intensities can be described by eq 1 and is governed by T_{CP}, the cross-polarization time constant, which controls the signal build up, and $T_{1\rho}^H$, the proton spin lattice relaxation time in the rotating frame, which controls the signal decay [22].

$$I_{(t)} = \frac{I_0}{1 - \frac{T_{CP}}{T_{1\rho}^H}} \left[\exp\left(-\frac{t}{T_{1\rho}^H}\right) - \exp\left(-\frac{t}{T_{CP}}\right) \right]. \qquad (1)$$

I_0 and $I_{(t)}$ are the initial intensity and intensity at contact time t. T_{CP} depends on the ^{1}H-^{29}Si distance and the number of protons in the vicinity of ^{29}Si, with shorter distances and a greater number of protons reducing T_{CP}. $T_{1\rho}^H$ is controlled by molecular motion at frequencies of 10^4–10^5 Hz. For a brief review of CP theory, see ref 20.

Fitting the observed data with eq 1 yields the CP relaxation parameters, T_{CP} and $T_{1\rho}^H$ (Figure 4A and Table 2), and the results indicate that the CP behavior of the Q^1, Q^2, and Q^3 sites are different. The $T_{1\rho}^H$ value of

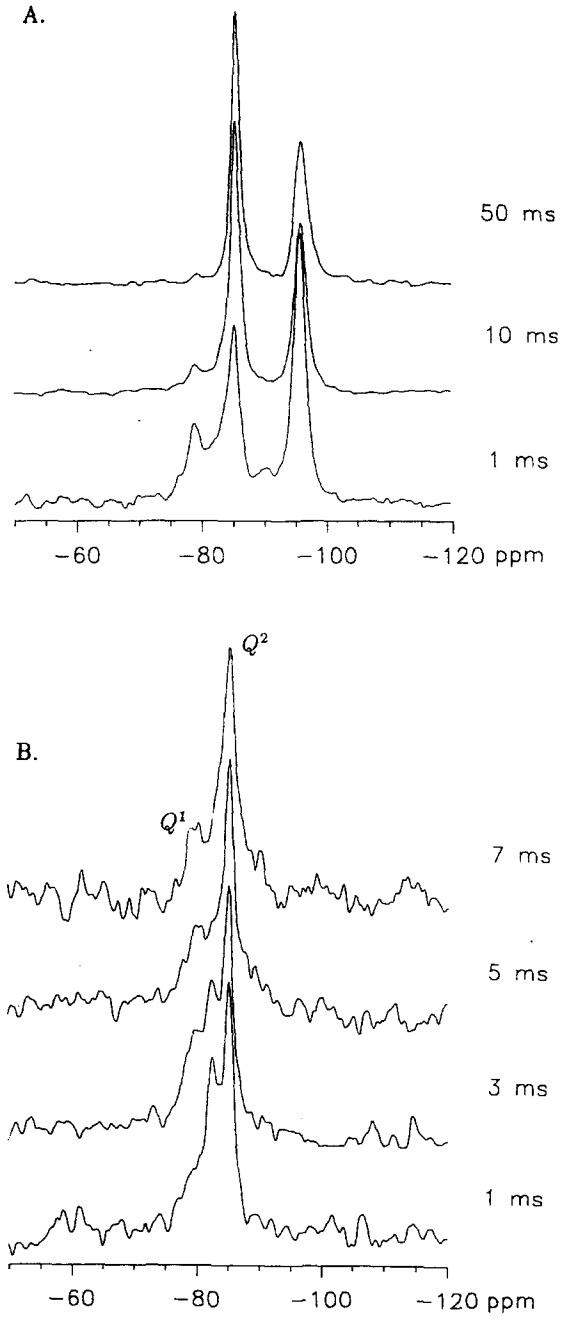

FIGURE 3. ^{1}H-^{29}Si CPMAS NMR spectra of directly synthesized 1.1-nm tobermorite (A) and jennite (B) with the indicated contact times.

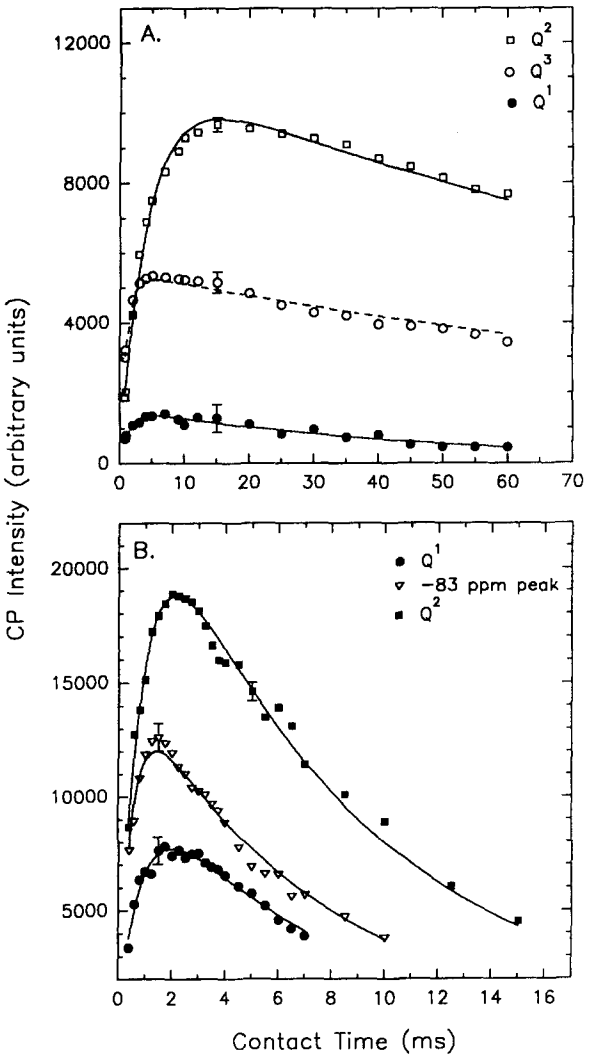

FIGURE 4. Dependence of cross-polarization intensity on contact time for directly synthesized 1.1-nm tobermorite (A) and jennite (B). The points are averages of at least two measurements of peak height. The curves are calculated based on eq 1, and the parameters are given in Table 2.

protons associated with Q^1 sites is about 48 ms, about one third that of the protons associated with Q^2 and Q^3 sites (150 ms for both). This large difference demonstrates that there are separate proton reservoirs in the structure, one associated with Q^1 sites only and the other associated with both the Q^2 and Q^3 sites. Significant spin diffusion occurs only within each reservoir but not between them. This is possible only when the two reservoirs are physically separated. We interpret this observation to indicate that most Q^1 sites are not on chain ends but in dimers separated from the chains and that the cross-linked chains are so long that the effects of the chain ends are negligible.

The T_{CP} values for the Q^1 and Q^3 sites are similar and much smaller than those of the Q^2 sites, indicating that CP is more effective for Q^1 and Q^3 sites than for Q^2 sites. The effectiveness of CP is proportional to both the number of protons in the vicinity of the Si and the ^{1}H-^{29}Si internuclear distance. Si-OH linkages are effective in this regard. In the ideal structure of tobermorite, BT's are the only sites that can be protonated (Si-OH) [3]. Cross-linking of BT only eliminates one of the two non-

TABLE 2. Summary of room temperature cross-polarized parameters for crystalline hydrous Ca-silicate phases

Samples		1.1-nm Tobermorite		Tobermorite (1.4 nm)	Jennite	Calcio chondrodite	Hillebrandite
		Dir.	Indir.				
Q^0	T_{CP}					7.3	
(±10%)	$T_{1\rho}^H$					933.4	
Q^1	T_{CP}	1.5			0.9		
(±10%)	$T_{1\rho}^H$	48.7			6.5		
Q^2	T_{CP}	4.2	0.7	0.7	0.9		3.3
(±10%)	$T_{1\rho}^H$	150.0	13.7	9.8	8.1		46.6
Q^3	T_{CP}	1.1					
(±10%)	$T_{1\rho}^H$	150.0					
−83 ppm	T_{CP}				0.5		
(±10%)	$T_{1\rho}^H$				6.9		
S/N		134.3	20.6	9.3	16.5	131.5	99.5

The T_{CP} and $T_{1\rho}^H$ values are based on curve fitting of the contact time dependence data and are both in units of millisecond. The signal to noise (S/N) ratios given are the largest observed in the CPMAS spectra of each sample. Dir. represents directly synthesized 1.1-nm tobermorite. Indir. represents 1.1-nm tobermorite formed by heating 1.4-nm tobermorite at 105°C.

bridging oxygen (NBO) sites, and the other one may be protonated (Si-OH). Si-OH linkages may also form on one of the three NBO's of the Q^1 sites. Therefore, it is possible that the greater average T_{CP} value of Q^2 sites is due to the lack of directly bonded OH^- groups on them.

The CPMAS spectra of the 1.1-nm tobermorite sample obtained by heating are also similar to its MAS NMR spectrum, but the CP relaxation parameters and the signal to noise (S/N) ratios are much smaller than those of the directly synthesized (Table 2). The smaller $T_{1\rho}^H$ indicates that there is more proton motion in the 10^4–10^5 Hz frequency range in the heated sample. Thus, the cross-linking in the directly synthesized 1.1-nm tobermorite seems to result in a more rigid structure. The larger S/N ratios of the CP spectra of this sample are also consistent with this idea.

^{17}O MAS NMR. The ^{17}O MAS NMR spectra of the ^{17}O-exchanged 1.1-nm tobermorite samples are similar and contain multiple peaks, a narrow one located at ca. 103 ppm and broad, overlapping components between 80 and −50 ppm (Figure 5A and B). There are 18 different O sites in ideal 1.1-nm tobermorite [3], but because of peak overlap these sites cannot be resolved. Consequently, the peaks can be assigned to only different local bonding arrangements. Assignment of the peaks and the deconvolution of the spectra must be based on the results of model compounds with known structures. Previous work on C-S-H [23] and various oxides and silicates [24–28] provides good starting parameters. ^{17}O MAS NMR spectra we collected for silica gel (Si-OH), portlandite (Ca-OH), and Ca-silicate glasses [bridging oxygen (BO) and NBO] [19] also provide references for the deconvolution.

The ^{17}O MAS NMR spectra of both 1.1-nm tobermorite specimens can be simulated with a six-site model (Figure 5A and B and Table 3), but the local structural environments of the different sites may be different in the two specimens. There are two NBO sites with different chemical shifts. We assign the main peak at 104 ppm to NBO sites bonding to one Si and two Ca^{2+}'s (Si-O-2Ca), which are the only NBO sites present in the ideal structure [3]. The second NBO site has a maximum at 89 ppm and is assignable to oxygens bonding to one Si and three Ca^{2+}'s (Si-O-3Ca). Such NBO sites do not exist in the ideal structure of 1.1-nm tobermorite but occur in many Ca-silicates including xonotlite and foshagite [25,29,30]. The general principle that chemical shifts become more shielded (less positive) with increasing nearest neighbor coordination number [31] supports these assignments.

The parameters for Ca-OH sites [quadrupolar coupling constant (QCC), η, and δi] obtained from the simulation are similar to those of portlandite, indicating a similar local structural environment. Ca-OH sites in portlandite are tetrahedrally coordinated by a proton and three Ca^{2+}'s [32]. Similar coordination for these sites may also occur in 1.1-nm tobermorite.

There are three different kinds of BO sites in ideal 1.1-nm tobermorite [3]. But due to the disorder and increased polymerization of our samples, we have simulated the spectra with only one BO site using parameters similar to those for Ca-silicate glasses [19].

The parameters we used for Si-OH sites are similar to those previously reported for Si-OH sites in $(C_6H_5)_2SiOH$ [33]. Whether there is additional Ca^{2+} bonded to this O site is not clear due to the unknown positions of

Advn Cem Bas Mat
1996;3:133-143

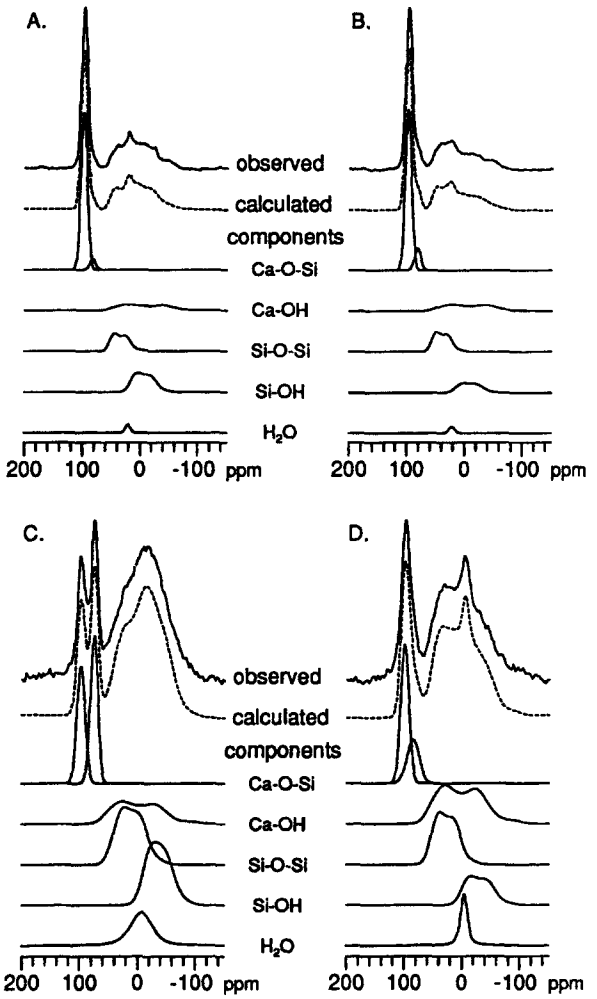

FIGURE 5. Observed and simulated ^{17}O MAS NMR spectrum of 1.1-nm tobermorite made by direct synthesis (A), and by heating of 1.4-nm tobermorite at 105°C for 12 hours (B), 1.4-nm tobermorite (C), and jennite (D). The component peaks are calculated based on the parameters listed in Table 3.

protons in the refined structure and the clear difference between the refined structure and real structures of our samples. However, based on the coordinations of other O sites in Ca-silicates, it is possible that one or two Ca^{2+}'s may be bonded to this site.

The spectral simulations require a relatively narrow peak near 20 ppm, and we assign this peak to molecular water. Liquid water at room temperature resonates at 0 ppm, but larger positive chemical shifts are not impossible [34].

The simulated relative intensities of the peaks for different sites may not reflect the actual site abundances due to problems associated with fitting multiple overlapping peaks, possible signal loss for broad peaks, and possible differential site exchange. Thus, the simulations are not unique, but they are consistent with the ^{29}Si NMR results in that NBO sites have the largest relative intensity.

1.4-nm Tobermorite

^{29}Si MAS NMR. The ^{29}Si MAS NMR spectrum of our 1.4-nm tobermorite is dominated by a Q^2 peak at −85 ppm (Figure 1C). The relative intensity near −80 ppm (Q^1) is less than 5%. Thus, the structure of this phase contains primarily single silicate chains, consistent with previous reports [4,8].

The crystal structure of 1.4-nm tobermorite, $Ca_5(Si_6O_{18}H_2) \cdot 8H_2O$, has not been solved but is thought to be similar to that of 1.1-nm tobermorite with more water molecules in the interlayer [1], consistent with NMR results. Based on a single-chain structure (Q^2) and the known C/S ratio, we calculate that about 26% of the Ca atoms occur in the interlayer, because only paring tetrahedra (PT) of the dreierkettens are directly bonded to the CaO layers.

^1H-^{29}Si CPMAS NMR. The ^1H-^{29}Si CPMAS NMR spectra of the 1.4-nm tobermorite have very low S/N ratios (<9.3) and contain peaks for both Q^2 and Q^1 sites. The relative intensities for the Q^1 peaks are much greater than in the MAS spectrum and vary little with contact time, consistent with the presence of more protons in the vicinity of Q^1 sites than Q^2 sites. Quantitative analysis of the Q^1 peaks is impossible due to the low S/N ratios.

The dependence of the CP intensity on contact time for the Q^2 sites can be fit well with eq 1, and the T_{CP} and $T_{1\rho}^H$ values are much smaller than those of the directly synthesized 1.1-nm tobermorite but are comparable with those of the 1.1-nm tobermorite obtained by heating the 1.4-nm tobermorite (Table 2). The small $T_{1\rho}^H$ value (9.85 ms) probably indicates relatively strong proton motion at frequencies in the 10^4–10^5 Hz range [35]. This motion destroys the coupling between protons and silicons, resulting in inefficient CP, and is also the reason of the low S/N ratios of the CP spectra.

^{17}O MAS NMR. The ^{17}O MAS NMR spectrum of 1.4-nm tobermorite is similar to those of the 1.1-nm tobermorites but contains more intensity in the 60 to −80 ppm region and two well-separated peaks in the NBO region (Figure 5C). As for the 1.1-nm tobermorites, the spectrum can be simulated with a six-site model. The two narrow peaks located at about 106 and 83 ppm can both be assigned to NBO sites with the one at 106 due to Si-O-2Ca sites and the one at 83 ppm due to Si-O-3Ca sites. The rest of the spectrum is due to BO sites, Ca-OH, Si-OH, and H_2O (Table 3).

The ^{17}O data are consistent with the ^{29}Si data within the experimental errors. The 1.4-nm tobermorite has a C/S ratio of 0.9 and contains single silicate chains (Q^2 sites only). There are one BO and two NBO's per Q^2 site. For the structure to be electrically neutral, the NBOs must be charge balanced by either Ca^{2+} or H^-. If all the NBO's are charge balanced by Ca^{2+}, there are two Si-

TABLE 3. Quadrupolar coupling constant (QCC), asymmetry parameter (η, and isotropic chemical shift (δ_i of different ^{17}O sites in hydrous Ca-silicate phases

Sample	^{17}O Sites	QCC (MHz) (±1)	η (±0.5)	δ_i (ppm) (±5)	Intensity (%) (±10%)
	Si-O-2Ca	1.8 (1.8)	0.2 (0.2)	104 (104)	47.0 (48.6)
	SI-O-3Ca	1.9 (2.0)	0.2 (0.2)	89 (89)	3.0 (6.7)
Tobermorite	Ca-OH	7.6 (7.6)	0.3 (0.3)	67 (68)	13.3 (15.3)
(1.1-nm)	BO	4.4 (4.3)	0.0 (0.0)	59 (62)	14.8 (16.7)
	Si-OH	4.8 (4.9)	0.0 (0.0)	23 (21)	20.1 (10.9)
	H_2O	0.0 (0.0)	0.0 (0.0)	20 (21)	1.8 (1.8)
	Si-O-2Ca	2.1	0.2	106	12.6
	Si-O-3Ca	2.0	0.2	83	15.0
Tobermorite	Ca-OH	7.4	0.3	72	15.0
(1.4-nm)	BO	5.4	0.0	49	22.8
	Si-OH	5.0	0.0	−4	22.5
	H_2O	0.0	0.0	−7	12.1
	NBO	2.0	0.2	107	18.7
	NBO	2.4	0.2	95	8.6
Jennite	Ca-OH	7.3	0.3	73	29.7
	BO	5.1	0.0	61	21.8
	Si-OH	5.4	0.0	9	13.7
	H_2O	0.0	0.0	−4	7.6
Calcio	NBO	2.0	0.2	129	55.2
chondrodite	NBO	2.0	0.2	109	44.8
Hillebrandite	NBO			106[a]	

There are two sets of data for 1.1-nm tobermorite, the one in parenthesis is for 1.1-nm tobermorite obtained by heating 1.4-nm tobermorite at 105°C, and the other is for directly synthesized sample. BO = bridging oxygen; NBO = nonbridging oxygen.
[a]Peak maximum.

O-Ca linkages required per tetrahedron. But at the 0.9 C/S ratio, Ca^{2+}'s can only balance 1.8 NBO's, and the remaining 0.2 NBO's must form Si-OH linkages. Thus, the relative intensities of BO, Si-O-Ca, and Si-OH sites should be 33%, 60%, and 6% respectively. The simulated relative intensity for BO sites is 26% (normalized to 0% H_2O), consistent with the ^{29}Si NMR data. But the simulated relative intensities for the NBOs is 28% and that for the Si-OH linkages is 23%. Thus, assuming the spectra are quantitative, a portion of the Ca^{2+} does not charge balance the NBO's but rather forms Ca-OH linkages. Consequently, the unbalanced NBO's must form Si-OH linkages, resulting in a greater relative intensity for Si-OH sites.

The ^{17}O NMR data support the idea that the structures of 1.1- and 1.4-nm tobermorite are similar and provide a basis for analysis of their differences. Compared to the ideal structure of 1.1-nm tobermorite, the CaO layer in 1.4-nm tobermorite may be distorted due to the fact that more than half of the NBO's are bonded to three Ca^{2+}'s instead of two. The chemical shifts of the BO sites are also more shielded than that of 1.1-nm tobermorite. As in 1.1-nm tobermorite, there may be multiple, unresolvable BO sites in 1.4-nm tobermorite. The more shielded chemical shifts of these BO sites in 1.4-nm tobermorite may be caused by a greater average coordination to these sites by Ca^{2+}'s.

The ^{17}O and ^{29}Si NMR data are consistent with the idea that all oxygens in the CaO layer are shared with silicate chains [1], because it is possible to assign almost all the Ca-OH sites in the interlayer. As discussed previously, 26% of the Ca^{2+} occurs in the interlayer, and ^{17}O NMR data indicate that 35% of the Ca^{2+} occurs as Ca-OH sites. Therefore, only 9% of the Ca^{2+} in the main CaO layer occurs in Ca-OH linkages, which corresponds to only 4% of total O-sites.

Jennite

^{29}Si MAS NMR. The ^{29}Si MAS NMR spectrum of synthetic jennite is similar to that of 1.4-nm tobermorite and contains essentially only Q^2 sites (Figure 1D), corresponding to single silicate chains in the structure. This result contrasts with that of Komarneni et al. [8], who reported about 40% of Q^1 sites in addition to Q^2 sites for a synthetic jennite with a starting C/S ratio of 1. Their sample, if pure, must be highly disordered because the C/S ratio they used is too low for ideal jennite, which has C/S = 1.5 [14]. Thus, our sample appears to be a better representative of jennite.

Jennite is considered to have the ionic constitution $Ca_9(Si_6O_{18}H_2)(OH)_8 \cdot 6H_2O$ [14,36], but its structure has not been solved. The XRD data and thermal behavior [13,14] show that it has a layer structure and contains dreierkettens. It has been suggested that corrugated

Advn Cem Bas Mat
1996;3:133–143

central CaO layers are sandwiched between silicate chains and rows of OH^- groups [1]. The main difference between the proposed jennite structure and that of tobermorite is that in jennite half of the chains are alternately replaced by rows of OH^+ groups, resulting in a much larger *a* axis (0.996 nm). Although the proposed structure must be considered speculative, the ^{29}Si NMR data support it. Based on a single-chain structure and a C/S ratio of 1.4 (using the ideal C/S ratio of 1.5 yields the same conclusion), at least 28% of the Ca^{2+} must form Ca-OH linkages to maintain electrical neutrality, and the rest share oxygens with the silicate chains. However, the BT point into the interlayers, and there may not be many interlayer Ca^{2+}'s, considering the relatively small basal spacing (1.06 nm) [14]. If only PT's are bonded to Ca^{2+}'s, 48% of the Ca^{2+} is needed for charge balance and the rest forms Ca-OH linkages. BT can be charge balanced by formation of Si-OH linkages. Thus, the abundance of silicate tetrahedra and Ca-OH sites are roughly equal and can alternately occur in the structure.

^{1}H-^{29}Si CPMAS NMR. The ^{1}H-^{29}Si CPMAS NMR spectra of jennite are quite different than the MAS NMR spectrum. The Q^2 peak in the MAS spectrum is resolved into two narrow peaks at −85.3 and −82.7 ppm (Figure 3B). In addition, there are small peaks located at −80 ppm, corresponding to Q^1 sites. The relative intensities of the peaks can all be fit with eq 1 (Figure 4B).

The CP parameters of all three peaks are similar within experimental error and are smaller than those of directly synthesized 1.1-nm tobermorite but are comparable with those of 1.4-nm tobermorite (Table 2). The similarity of the $T_{1\rho}^H$ values for protons associated with Q^1 and Q^2 sites indicate that there is only one proton reservoir in the structure and, thus, that all three types of sites are near each other. Therefore, the Q^1 sites are most likely to be chain end tetrahedra due to missing BT rather than dimers in a different part of the structure. The −82.7 and −85.3 ppm peaks are both due to chain middle tetrahedra, but their local structural environments are different. The intensity decay of the −83 ppm peak appears not to be a single exponential, indicating that more than one site may contribute to it. There are two possibilities for the origin of two Q^2 sites in jennite. If the −85.3 ppm peak is due to the middle tetrahedra in dreierkettens similar to those in tobermorite, the −82.7 ppm peaks may be due to Si sites with different mean ∠SiOSi's or bonded to a different number of Ca^{2+}'s. Another possibility is that the dreierkettens in jennite are distorted so that the local structural environments of different tetrahedra, such as bridging and pairing tetrahedra, are different, resulting in different chemical shifts. Because NMR is primarily a local structural probe, it alone cannot resolve this issue, and the structure needs to be resolved from diffraction data.

There are two additional important observations concerning the ^{1}H-^{29}Si CPMAS data of jennite. The first one is that the protons in jennite are probably in motion at 10^4–10^5 Hz frequencies, because the $T_{1\rho}^H$ values for all three sites are very small and the S/N ratio is low (Table 2). However, the high concentration of OH^- groups and H_2O molecules also increase the efficiency of proton spin diffusion, reducing $T_{1\rho}^H$. Therefore, the proton motion may not be as important as in 1.4-nm tobermorite.

The second observation is that CP and ^{1}H-decoupling are very effective, indicating the proton motion does not fully destroy the ^{1}H-^{29}Si coupling, consistent with the first observation. Thus, the silicons and at least some protons are strongly coupled in jennite, resulting in the broad peak in the MAS NMR spectrum. This strong ^{1}H-^{29}Si coupling in jennite is exceptional among the crystalline phases discussed in this article and C-S-H gel discussed elsewhere [20]. This observation, the discussion of the last section, and the ^{17}O data shown below all lead to the conclusion that Si-OH linkages are present in jennite. This conclusion is the opposite of Komarneni et al. [8].

^{17}O MAS NMR. The ^{17}O MAS NMR spectrum of jennite is similar to that of 1.4-nm tobermorite except that the NBO peak near 95 ppm is much smaller and the water peak is more obvious and near 0 ppm (Figure 5D). Again, the spectrum can be fit relatively well with a six-site model, including two NBO sites, one Ca-OH site, one BO site, one Si-OH site, and H_2O (Table 3).

The chemical shift of the dominant NBO peak (107 ppm) is essentially the same as that of the 1.4-nm tobermorite and may also be due to the Si-O-2Ca sites, but the chemical shift of the weaker NBO peak (95 ppm) assignable to the Si-O-3Ca sites is more deshielded. However, because the two peaks are not as well separated as for 1.4-nm tobermorite, it is possible that there are more than two NBO sites, which may have the same nearest neighbor (NN) coordination but different bond lengths and angles and slightly different chemical shifts. In this case, it is not possible to distinguish between the NN coordination. Therefore, we assign the peaks simply to NBO sites.

The large relative intensity for Ca-OH sites demonstrates that many oxygens in the CaO layer are not shared with silicate chains but instead form Ca-OH sites, consistent with the proposed structure [1]. The chemical shift of the peak assigned to H_2O is about −4 ppm, much closer to 0 ppm than for tobermorite, consistent with the idea that its local environment is more like that of liquid water, probably due to hydrogen

bonding to the Ca-OH sites. The chemical shifts of the BO sites are similar to those of 1.1-nm tobermorite, whereas those of the Si-OH and H_2O sites are between the two tobermorites. It is likely that the local structural environments of different O sites in jennite are more or less similar to those of tobermorites, even though the long-range structure is different.

The ^{17}O NMR data are consistent with the ^{29}Si NMR data. Based on the calculations in the ^{29}Si section and only concerning charge balance, jennite should contain 53% NBOs, 26% BO's, and 21% Ca-OH. Only considering BO, NBO, and Ca-OH sites in the simulated spectrum, we obtain 35% NBO, 28% BO, and 38% Ca-OH sites, respectively. Comparing the results of the two methods, there are fewer NBOs and more Ca-OHs in the simulation, and the BOs are almost the same. This difference is consistent with the discussion in the ^{29}Si section that some of the Ca^{2+}s do not form NBOs but rather the Ca-OH sites in the main CaO layer. There are about 17% fewer NBOs in the simulation than in the idealized calculation, and this is coupled with a 17% increase in the Ca-OH sites. Consequently the same number of Si-OH linkages must occur to balance the charge. The simulation yields about 14% of Si-OH, agreeing well with the prediction. ^{17}O NMR data are also consistent with the idea that almost all Si-OH sites occur on BT sites, which yield 18% of Si-OH sites. The relative intensities of NBO and Ca-OH are similar, supporting the alternating occurrence of silicate chains and rows of OH^- groups. This also indicates that there are no interlayer Ca^{2+}'s because all Ca^{2+}'s occur in the main CaO layer.

Xonotlite

^{29}Si MAS NMR. The ^{29}Si MAS NMR spectrum of xonotlite is similar to that of the directly synthesized 1.1-nm tobermorite. It contains a Q^1 peak at −79.3 ppm, a Q^2 peak at −86.3 ppm, and two Q^3 peaks at −95.1 and −97.5 ppm (Figure 1E). The Q^2 peak is broad and asymmetrical to the left. This spectrum is slightly different than those previously reported [7,9], which contain no Q^1 peak and only one Q^3 peak.

The structure of xonotlite, $Ca_6Si_6O_{17}(OH)_2$, has been solved for different polytypes [29,37] and contains double dreierkettens (Si_6O_{17}) linked to CaO polyhedral sheets. The main structural difference between xonotlite and 1.1-nm tobermorite is that in xonotlite, the CaO polyhedral sheets are corrugated and split into ribbons so that the dreierkettens are connected with two CaO sheets of these ribbons and there is no interlayer region. Our results are consistent with the structure. However, our specimen appears to be highly disordered because it contains about 11% Q^1 and only 23% Q^3. Ideal xonotlite had 33.3% Q^3, 66.7% Q^2, and no Q^1 sites. The two peaks assignable to the Q^3 sites also indicate disorder for the cross-linking sites.

The ^{29}Si MAS NMR data indicate that the xonotlite sample is not Ca^{2+} deficient and does not require Si-OH linkages for charge balance, contrary to a previous report [38]. Charge balance calculations as described for 1.4-nm tobermorite and jennite indicate that our sample needs only a C/S ratio of 0.94 to maintain electrical neutrality, assuming that NBOs are preferentially charge balanced by Ca^{2+}. Ideal xonotlite would require a C/S ratio of 0.83 to maintain its charge balance. The theoretical C/S ratio of xonotlite is 1.0, and the extra Ca^{2+}'s form Ca-OH linkages.

^{1}H-^{29}Si MAS NMR. The ^{1}H-^{29}Si CPMAS NMR spectra of xonotlite are different than the MAS spectrum, because the Q^1 peak and the −95.1 ppm Q^3 peak are not present in the CP spectra at any contact time. The CP intensities of both the Q^2 and Q^3 peaks increase with increasing contact time up to 90 ms, and then decrease (Figure 6). This decrease may be an instrumental effect because the contact times are too long. The CP intensity oscillates with increasing contact time, but the oscillation cannot be simulated with the method developed by Müller et al. [39]. Thus, the oscillation is probably not due to Si-OH bonding but rather to multiple components in the proton spin system, such as both Ca-OH and H_2O.

The large CP intensities at long contact times indicate that the T_{CP} values must be large and that the ^{1}H–^{29}Si

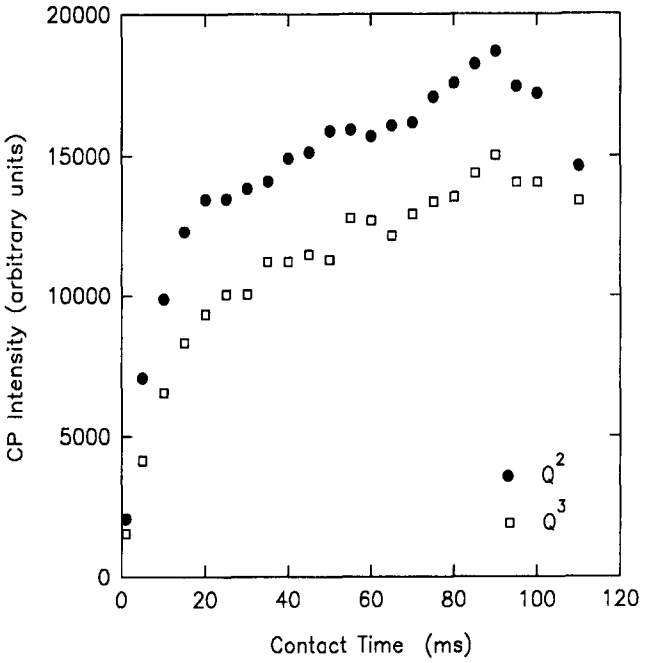

FIGURE 6. Dependence of cross-polarization intensity on contact time for xonotlite. The CP intensities are the average of at least two measurements of peak height.

Advn Cem Bas Mat
1996;3:133–143

distance may also be large. This result is consistent with the idea that there are no Si-OH linkages. The large CP intensities at long contact times also indicate that the $T_{1\rho}^{H}$ values are large, at least on the order of 100 ms. This large $T_{1\rho}^{H}$ indicates that there is little molecular motion at the 10^4–10^5 Hz range and that the proton concentration may be small, which decreases the efficiency of proton spin diffusion.

^{17}O exchange of xonotlite was not successful, and there is no detectable ^{17}O NMR signal.

Hillebrandite

^{29}Si MAS NMR. The ^{29}Si MAS NMR spectrum of hillebrandite contains only a Q^2 peak at −85.7 ppm, corresponding to single-chain structure (Figure 1F). This result is consistent with those previously reported [7,9,17].

The crystal structure of hillebrandite, $Ca_2SiO_3(OH)_2$, has recently been solved and contains a three-dimensional network of CaO polyhedra and a single Si_3O_8 dreierketten accommodated in the structural channels parallel to the a axis [40]. The ^{29}Si NMR data is consistent with this structure.

^{1}H-^{29}Si CPMAS NMR. The ^{1}H-^{29}Si CPMAS NMR spectra of hillebrandite is the same as the MAS spectrum and contains only a Q^2 peak. The CP intensity varies with contact time and can be well fit with eq 1 (Table 2). Compared with the CP relaxation data of other phases discussed in this article, the T_{CP} and $T_{1\rho}^{H}$ values for hillebrandite indicate that it has a relatively rigid structure but that the protons relax quickly via spin diffusion due to the abundant proton population. The CP data alone cannot confirm whether there are Si-OH linkages in the structure. Charge balance calculation indicates that no Si-OH linkages are required but that at least 50% of the Ca^{2+}must form Ca-OH linkages.

^{17}O MAS NMR. The ^{17}O MAS NMR spectrum of hillebrandite consists of a narrow peak with a maximum at *ca.* 106 ppm and poorly resolved intensity in the 60–0 ppm region (Figure 7). The 106 ppm peak can be assigned to the four NBO sites of hillebrandite, which are all bonded to one Si and three Ca^{2+}'s [40]. They cannot be further resolved due to the lack of quadrupolar line shape and peak overlap. The signal between *ca.* 60 and 0 ppm may be due to BO sites or Ca-OH linkages, but because of the low intensity, no reliable deconvolution can be achieved.

Calciochondrodite

^{29}Si MAS NMR. The ^{29}Si MAS NMR spectrum of calciochondrodite contains one peak at −72.7 ppm, corresponding to isolated tetrahedra, Q^0 sites (Figure 1G). This spectrum is consistent with that previously reported [9].

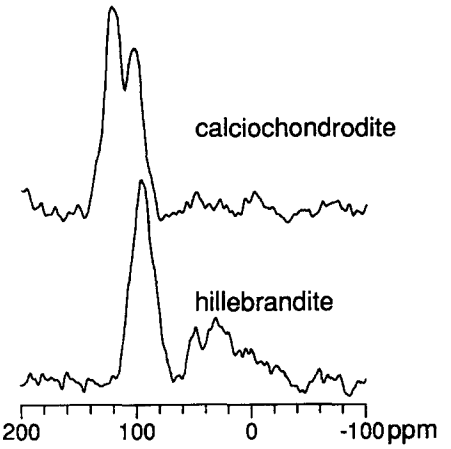

FIGURE 7. ^{17}O MAS NMR spectra of calciochondrodite and hillebrandite.

The crystal structure of calciochondrodite, $Ca_5(SiO_4)_2(OH)_2$, has been solved and contains portlandite-like layers between ideal Ca-olivine [41,42]. There is only one Q^0 Si site, consistent with the ^{29}Si NMR spectrum.

^{1}H-^{29}Si CPMAS NMR. The ^{1}H-^{29}Si CPMAS NMR spectra of calciochondrodite are the same as that of MAS spectrum, and the CP intensities increase with contact time, reach a maximum, and then decrease. The CP parameters obtained by fitting the intensities to eq 1 are larger than for the other phases examined (Table 2). The large T_{CP} value of 7.3 ms indicates a relatively large ^{29}Si–^{1}H distance, consistent with the structure with protons present only in the $Ca(OH)_2$ layers. The large $T_{1\rho}^{H}$ value of 933 ms indicates that there is little or no molecular motion at 10^4–10^5 Hz frequencies to facilitate proton relaxation. It is also consistent with a lower abundance of protons, in agreement with the composition.

^{17}O MAS NMR. The ^{17}O MAS NMR spectrum of calciochondrodite is quite different than those of tobermorite and jennite (Figure 7), and there are only two peaks located at 129 and 109 ppm assignable to NBO sites. In calciochondrodite, there are four crystallographically different O sites [41–43], two of them bonded to one Si and two Ca's and the other two bonded to one Si and three Ca's. The peak at 129 ppm can be assigned to the first two O sites and the peak at 109 ppm to the rest.

There is no intensity in the 60 to −60 ppm range, indicating that there are no BO and Si-OH sites, consistent, with the proposed structure. However, there is also no intensity assignable to Ca-OH sites, which should be present based on the structure. This inconsistency may be due to difficulty in ^{17}O exchange of the Ca-OH sites.

Acknowledgment

This project was done under the auspices of the Center for Advanced Cement Based Materials sponsored by the National Science Foundation and was supported by the grant DOE SBC NU YOUNG ANT.

References

1. Taylor, H.F.W. *Cement Chemistry.* Academic Press: London, 1990.
2. Taylor, H.F.W. *J. Am. Ceram. Soc.* **1986,** *69,* 464–467.
3. Hamid, S.A. *Zeit. Kristall.* **1981,** *154,* 189–198.
4. Wieker, W.; Grimmer, A.R.; Winkler, A.; Mägi, M.; Tarmak, M.; Lippmaa, E. *Cem. Concr. Res.* **1982,** *12,* 333–339.
5. Sato, H.; Grutzeck, M. *Mater. Res. Soc. Proc.* **1992,** *245,* 235–240.
6. Mitsuda, T.; Toraya, H.; Okada, Y.; Shimoda, M. *Ceram. Trans.* **1988,** *5,* 206–213.
7. Lippmaa, E.; Mägi, M.; Samoson, A.; Engelhardt, G.; Grimmer, A.R. *J. Am. Chem. Soc.* **1980,** *102,* 4889–4893.
8. Komarneni, S.; Roy, D.M.; Fyfe, C.A.; Kennedy, G.J. *Cem. Concr. Res.* **1987,** *17,* 891–895.
9. Bell, G.M.M.; Bensted, J.; Glasser, F.P.; Lachowksi, E.E.; Roberts, D.R.; Taylor, M.J. *Adv. Cem. Res.* **1990,** *3,* 23–37.
10. El-Hemaly, S.A.S.; Mitsuda, T.; Taylor, H.F.H. *Cem. Concr. Res.* **1977,** *7,* 429–438.
11. Chan, C.F.; Mitsuda, T. *Cem. Concr. Res.* **1978,** *8,* 135–138.
12. Hara, N.; Chan, C.F.; Mitsuda, T. *Cem. Concr. Res.* **1978,** *8,* 113–116.
13. Carpenter, A.B.; Chalmers, R.A.; Gard, J.A.; Speakman, K.; Taylor, H.F.W. *Am. Mineral.* **1966,** *51,* 56–74.
14. Gard, J.A.; Taylor, H.F.W.; Cliff, G.; Lorimer G.W. *Am. Mineral.* **1977,** *62,* 365–368.
15. Hara, H.; Inous, N. *Cem. Concr. Res.* **1980,** *10,* 677–682.
16. Taylor, H.F.W. *The Chemistry of Cement,* vol. 1. Academic Press: London, 1964.
17. Ishida, H.; Mabuchi, K.; Sasaki, K.; Mitsuda, T. *J. Am. Ceram. Soc.* **1992,** *75,* 2427–2432.
18. Cong, X.; Kirkpatrick, R.J. *Adv. Cem. Based Mater.* **1996,** *3,* 144–156.
19. Cong, X.; Kirkpatrick, R.J. *J. Am Ceram. Soc.*, in press.
20. Cong, X.; Kirkpatrick, R.J. *Adv. Cem. Res.* **1995,** *7,* 103–112.
21. Mitsuda, T.; Taylor, H.F.W. *Mineral. Mag.* **1978,** *42,* 229–235.
22. Mehring, M. *Principles of High Resolution NMR in Solids.* Springer-Verlag: Berlin, 1983.
23. Cong, X.; Kirkpatrick, R.J. *Cem. Concr. Res.* **1993,** *23,* 1065–1077.
24. Turner, G.L.; Chung, S.E.; Oldfield, E. *J. Magn. Reson.* **1985,** *64,* 316–324.
25. Timken, H.K.C.,; Schramm, S.E.; Kirkpatrick, R.J.; Oldfield, E. *J. Phys. Chem.* **1987,** *91,* 1054–1058.
26. Schramm, S.; Kirkpatrick, R.J.; Oldfield, E. *J. Am. Chem. Soc.* **1983,** *105,* 2483–2485.
27. Schramm, S.; Oldfield, E. *J. Am. Chem. Soc.* **1984,** *106,* 2502–2506.
28. Kirkpatrick, R.J.; Dunn, T.; Schramm, S.; Smith, K.A.; Oestrike, R.; Turner, G. In *Structure and Bonding in Noncrystalline Solids,* Walrafen, G.E., Revesz, A.G., Eds. Plenum Press: New York, 1986; pp 303–327.
29. Kudoh, Y.; Takeuchi, Y. *Mineral. J.* **1979,** *9,* 349–373.
30. Gard, J.A.; Taylor, H.F.W. *Acta Cryst.* **1960,** *13,* 785–793.
31. Harris, R.K. *Nuclear Magnetic Resonance Spectroscopy.* Longman Scientific & Technical: New York, 1986.
32. Henderson, E.; Bailey, J.E. *J. Mater. Sci.* **1988,** *23,* 501–508.
33. Walter, T.H. *Multinuclear Solid-State NMR Studies of Supported Transition Metal Carbonyls,* PhD Thesis. University of Illinois at Urbana-Champaign, 1988.
34. Spiess, H.W.; Garrett, B.B.; Sheline, R.K.; Rabideau, S.W. *J. Chem. Phys.* **1969,** *51,* 1201–1205.
35. McCall, D.W. *Acc. Chem. Res.* **1971,** *4,* 223–232.
36. Kusachi, I.; Henmi, C.; Henmi, K. *Mineral. J.* **1989,** *14,* 279–292.
37. Mamedov, K.H.S.; Belov, N.V. *Dok. Akad. Nauk SSSR* **1955,** *104,* 615–618.
38. Kalousek, G.L.; Mitsuda, T,; Taylor, H.F.W. *Cem. Concr. Res.* **1977,** *7,* 305–312.
39. Müller, L., Kumar, A.; Baumann, T.; Ernst, R.R. *Phys. Rev. Lett.* **1974,** *32,* 1402–1406.
40. Dai, Y.; Post, J.E. *Am. Mineral.* **1995,** *80,* 841–844.
41. Ganiev, R.M.; Kharitonov, Y.A.; Ilyukhin, V.V.; Belov, A.N.V. *Sov. Phys. Dokl.* **1970,** *14,* 946–948.
42. Kuznetsova, T.P.; Nevskii, N.N.; Ilyukhin, V.V.; Belov, N.V. *Sov. Phys. Crystallogr.* **1980,** *25,* 91–92.
43. Kirfel, A.; Hamm, H.-M.; Will, G. *Tschermaks Min. Petr. Mitt.* **1983,** *31,* 137–150.